Intelligent and Converged Networks
2023, 4(1): 28−40

ISSN 2708-6240
DOI: 10.23919/ICN.2023.0003

Online search for UAV relay placement for free-space optical communication under shadowing

Yuanshuai Zheng, Yinjun Wang, and Junting Chen*

Abstract: Unmanned aerial vehicle (UAV) relaying is promising to overcome the challenge of signal blockage in free-space optical (FSO) communications for users in dense urban area. Existing works on UAV relay placement are mostly based on simplified line-of-sight (LOS) channel models or probabilistic channel models, and thus fail to capture the actual LOS status of the optical communication link. By contrast, this paper studies three-dimensional (3D) online placement for a UAV to construct relay links to two ground users in deep shadow with LOS guarantees. By analyzing the properties of the UAV relay placement problem, it is found that searching on a plane that approximates the equipotential surface can achieve a good performance and complexity trade-off for a good placement of the UAV relay in 3D. Based on these insights, a two-stage online search algorithm on an equipotential plane (TOSEP) is developed for a special case where the equipotential surface turns out to be an equipotential plane. For the general case, a strategy called gradient projected online search algorithm on an approximated equipotential plane (GOSAEP) is developed, which approximates the equipotential surface with a perpendicular plane using the gradient projection method. Numerical experiments are conducted over a real-world city topology, and it is shown that the GOSAEP achieves over 95% of the performance of the exhaustive 3D search scheme within a 300-m search length.

Key words: free-space optical communication; relay communication; unmanned aerial vehicle (UAV); trajectory design; capacity maximization

1 Introduction

Free-space optical (FSO) communication has been widely considered as a trending technology for establishing high-capacity and cost-efficient links with high-level physical layer security in emerging wireless networks[1−3]. However, one of the most significant limitations of FSO communications is its vulnerability to signal blockage. As a result, FSO communications require a line-of-sight (LOS) condition between a transmitter and a receiver[4, 5], which imposes a stringent requirement in the application in a dense urban environment where FSO links are likely to be obstructed by buildings and vegetation[6−8].

Unmanned aerial vehicle (UAV) relays have the potential to circumvent the challenge imposed by signal blockage for FSO communications. When the direct communication link of two FSO terminals is blocked, UAV can serve as an aerial relay to establish LOS links for these two terminals. In particular, it becomes easier to establish an LOS condition from the air, and in addition, UAV relays can dynamically adjust its position according to the positions of the mobile terminals. As such, in comparison to traditional fixed-position base stations (BSs), the UAV-aided network can respond quickly to occasional and temporary service requests from users in deep shadow[9, 10].

Despite many studies in the area of spatial deployment of UAVs, there are still numerous difficulties. First, most existing works[11−17] on UAV

• Yuanshuai Zheng, Yinjun Wang, and Junting Chen are with the School of Science and Engineering and the Future Network of Intelligence Institute (FNii), The Chinese University of Hong Kong, Shenzhen 518172, China. E-mail: yuanshuaizheng@link.cuhk.edu.cn; yinjunwang@link.cuhk.edu.cn; juntingc@cuhk.edu.cn.
* To whom correspondence should be addressed.
Manuscript received: 2022-11-20; revised: 2023-02-10; accepted: 2023-03-15

placement focus on the UAV position optimization in 2D with a fixed altitude from the ground, and therefore, the existing solutions did not unleash the great potential of UAV relaying in 3D. For example, allowing adjustments to the altitude of the UAV may significantly increase the chance of discovering the LOS positions while maintaining a short distance to both ground terminals. Second, many existing works considered simplified terrain models, such as stochastic terrain models[18, 19] or simplified analytic geometry models[20, 21]. These simplified models fail to capture the actual propagation condition of the terrain in real life, which may consist of arbitrary structures with a great variety in shapes and locations. Thus, the solutions based on the simplified terrain model cannot guarantee LOS conditions for FSO communications in real environment.

Specifically, to simplify the UAV placement problem and make the problem more trackable, the works[22, 23] adopted pure LOS channel models, assuming no obstacles from the environment. The probabilistic LOS channel models were used to depict the effect of the blockage in Refs. [24−29]. Since the pure LOS channel models and probabilistic channel models are over-simplified, they fail to capture the real distribution of the obstacles, and thus, they cannot guarantee the LOS conditions of the UAV positions.

To account for the effect of the real-world environment on signal obstruction, Refs. [30, 31] proposed using radio maps, which are built from a large number of real-world channel measurements, to aid in UAV placement or path planning. The work[32] used radio maps to jointly optimize the UAV position, user equipment association, and backhaul capacity allocation, which is a challenging mixed non-convex and combinatorial problem. However, the optimality in Ref. [32] was still not guaranteed. Although radio maps are capable of capturing the realistic channel gain, collecting a substantial amount of channel data is time-consuming, but necessary for creating a radio map. In comparison to radio maps, 3D coverage maps are more readily available and widely used in the works[20, 25, 33, 34]. The work[20] used the analytic geometry methods to model the obstructed regions, and employed Lagrangian relaxation to streamline the UAV placement issue. While the optimality was still debatable, a two-loop iterative technique to solve the Lagrangian problem was developed in Ref. [20]. The authors of Ref. [25] used a map compression method to utilize raw map data, and obtained a local optimal solution to a path planning problem. Based on local digital elevation model (DEM) data, Ref. [33] developed a geometric method to predict the transmission conditions and proposed a greedy user scheduling algorithm with geometric analysis. Reference [34] presented a greedy approach where the trajectory is designed locally and piece by piece based on the 3D map. To sum up, the map-based approaches are still very limited. On one hand, the acquisition of fine-grained map data remains costly. The 3D map-aided approaches, on the other hand, are heavily reliant on the freshness of the map data. Outdated map data may still cause issues with practical implementation.

This paper focuses on the 3D placement of a UAV relay for the FSO communication system between two ground users in dense urban area, with an objective to maximize worse relay link between the UAV and the two ground users. Note that it is assumed that there is no prior geometric information, and thus, online search is significantly preferred. In our prior work[35], a 2D online search algorithm with guaranteed LOS conditions is developed. However, the search algorithm on the middle perpendicular plane in Ref. [35] requires the UAV to move along dynamically adjusted curves, resulting in difficulties of implementation and possible loss of accuracy. On the contrary, Algorithm 1, as a benchmark algorithm, proposed in this paper is much easier to implement and has lower complexity due to the simpler movement patterns and tighter stopping criterion. Moreover, Algorithm 1 is theoretically proved to find the optimal relay position on an equipotential plane between two users in a special case. For the general case, i.e., the relay channels could be different from each other, the equipotential surface is curved and it is challenging to search on such a curved equipotential surface. Exploiting the properties of the equipotential surfaces, we develop a strategy to select the best perpendicular plane for approximating the curved equipotential surface, and then search on such a

Algorithm 1 TOSEP

Input: User positions $\boldsymbol{u}_1$, $\boldsymbol{u}_2$, and a step size μ.

Output: The optimal relay position $\hat{\boldsymbol{x}}$

1. Find an SLOS position $\boldsymbol{x}_0 \in \mathcal{D}_1 \cap l_0$ on $\mathcal{M}_0$ by increasing the altitude of UAV.
2. Initialize $\hat{\boldsymbol{x}} \leftarrow \boldsymbol{x}_0$ and $\boldsymbol{x} \leftarrow \boldsymbol{x}_0$.
3. **Stage 1**: Conduct search on the left side of l_0 on $\mathcal{M}_0$:
   (1) If $\boldsymbol{x} \in \mathcal{D}_1 \cap \mathcal{M}_0$, then,
   (a) If $F(\boldsymbol{x}) > F(\hat{\boldsymbol{x}})$, update $\hat{\boldsymbol{x}} \leftarrow \boldsymbol{x}$ and $r(\hat{\boldsymbol{x}})$ according to Eq. (8).
   (b) $\boldsymbol{x} \leftarrow \boldsymbol{x} + \Delta\boldsymbol{x}_1$, where $\Delta\boldsymbol{x}_1 = (0, 0, -\mu)$.
   (2) If $\boldsymbol{x} \in \mathcal{D}_2 \cap \mathcal{M}_0$, update $\boldsymbol{x} \leftarrow \boldsymbol{x} + \Delta\boldsymbol{x}_2$, where $\Delta\boldsymbol{x}_2 = (-\mu, 0, 0)$.
   (3) Repeat Steps (1) and (2) until $|x_1| > r(\hat{\boldsymbol{x}})$ or $|x_3| < H_{\min}$.
4. **Stage 2**: Conduct search on the right side of l_0 on $\mathcal{M}_0$: Start again from $\boldsymbol{x}_0$. Repeat Steps (1)–(3), but replace $\Delta\boldsymbol{x}_2$ by $\Delta\boldsymbol{x}_2 = (\mu, 0, 0)$.

perpendicular plane to find the best relay position.

In summary, the contributions of this paper are as follows:

(1) We formulate a generalized optimal UAV relay placement problem in an FSO communication system. Two solution properties are elucidated, providing a foundation for searching for the optimal position online.

(2) A two-stage online search algorithm on an equipotential plane (TOSEP) with theoretically guaranteed optimality on the search plane is developed. In addition, the trajectory length is proved to be upper bounded by a linear function of the initial altitude.

(3) Exploiting the properties of general equipotential surfaces, we propose a gradient projected online search algorithm on an approximated equipotential plane (GOSAEP). The GOSAEP also has a 2D optimality guarantee and a linear search length.

(4) The experiments are conducted on real-world map data. The numerical results show that the GOSAEP achieves above 95% to the exhaustive 3D search scheme within a 300-m search distance under all tested general cases.

2 System model

2.1 Property of the free-space optical air-to-ground propagation

Consider a UAV located at $\boldsymbol{x} = (x_1, x_2, x_3) \in \mathbb{R}^3$ that relays signals between User 1 located at $\boldsymbol{u}_1 \in \mathbb{R}^3$ and User 2 located at $\boldsymbol{u}_2 \in \mathbb{R}^3$. Let $\mathcal{D} = \{\boldsymbol{x} \in \mathbb{R}^3 | x_3 \geqslant H_{\min}\}$ be the domain of all possible UAV positions where $H_{\min}$ is required to be larger than the highest terrain altitude. Consider a partition of $\mathcal{D}$ into two disjoint segments according to the propagation environment around $\boldsymbol{u}_i$, i.e., $\mathcal{D} = \mathcal{D}_1^{(1)} \cup \mathcal{D}_2^{(1)} = \mathcal{D}_1^{(2)} \cup \mathcal{D}_2^{(2)}$ where $\mathcal{D}_1^{(i)}$ is the LOS segment, and $\mathcal{D}_2^{(i)}$ is the non-line-of-sight (NLOS) segment with respect to (w.r.t.) the i-th user. To make the analysis mathematically tractable, the propagation segments are assumed to be nested: Increasing the altitude of the UAV lowers the degree of signal obstruction, i.e., for any $(x_1, x_2, x_3) \in \mathcal{D}_j^{(i)}$ and $(x_1, x_2, x_3') \in \mathcal{D}_k^{(i)}$, it holds that if $x_3' > x_3$, then, $j \geqslant k$ where $j \in \{1, 2\}$ and $k \in \{1, 2\}$. The above property is named as *LOS property of nested propagation segments*.

2.2 Capacity maximization

Consider a decode-and-forward (DF) relay system where the UAV serves as a relay to two obstructed users. Denote the channel gain of the source-to-relay (SR) channel, i.e., User 1 to UAV, and the relay-to-destination (RD) channel, i.e., UAV to User 2, as $g_{\mathrm{s,r}}$ and $g_{\mathrm{r,d}}$, respectively. According to Ref. [23], $g_{\mathrm{s,r}}$ and $g_{\mathrm{r,d}}$ are specified as

$$g_{\mathrm{s,r}} = \beta_0 / \|\boldsymbol{x} - \boldsymbol{u}_1\|^{\alpha_0} \tag{1}$$

$$g_{\mathrm{r,d}} = \beta_0 / \|\boldsymbol{x} - \boldsymbol{u}_2\|^{\alpha_0} \tag{2}$$

where α_0 and β_0 are the channel parameters of LOS links. Note that in this paper, LOS channels are required due to the intolerant attenuation of NLOS links in FSO communications. Since shadowing fading has little effect on LOS channels, it is not considered here[20, 36].

Then, the end-to-end capacity of such a DF system can be modeled as

$$\begin{aligned} C_{\mathrm{DF}} = \min\{&W_{\mathrm{s}} \log_2(1 + P_{\mathrm{s}} g_{\mathrm{s,r}} / N_0), \\ &W_{\mathrm{r}} \log_2(1 + P_{\mathrm{r}} g_{\mathrm{r,d}} / N_0)\} \end{aligned} \tag{3}$$

where W_{s} is the channel bandwidth of the SR channel, W_{r} is the channel bandwidth of the RD channel, P_{s} and P_{r} represent the transmission power of User 1 and the UAV, respectively, and N_0 is the noise power. Obviously, to maximize the performance of the relay

system, one needs to maximize C_{DF}.

2.3 Problem formulation

The generalized formulation is obtained from the above capacity maximization model. Consider the i-th user's link performance wherein the objective function is composed of two different sub-objective functions $f_k^{(i)}$, indexed by k, where $k \in \{1,2\}$ refers to the segment in which the UAV is located, i.e., $\boldsymbol{x} \in \mathcal{D}_k^{(i)}$. Denote the distance between the i-th user and the UAV as $d_i(\boldsymbol{x}) = \|\boldsymbol{x} - \boldsymbol{u}_i\|_2$. It is assumed that $f_k^{(i)}(d_i(\boldsymbol{x}))$ is decreasing and differentiable w.r.t. $d_i(\boldsymbol{x})$. To make each link's performance function more compact, an indicator function is introduced as below

$$II(A) = \begin{cases} 1, & A \text{ is satisfied;} \\ 0, & \text{otherwise} \end{cases} \tag{4}$$

Then, the i-th user's link performance function can be formulated as

$$F^{(i)}(\boldsymbol{x}) = \sum_{k=1}^{2} f_k^{(i)}(d_i(\boldsymbol{x})) \cdot II\{\boldsymbol{x} \in \mathcal{D}_k^{(i)}\} \tag{5}$$

To maximize the capacity of the UAV relay system, the performance of the worse channel between the SR channel and the RD channel should be maximized. Specifically, the problem can be formulated as

$$\begin{aligned} \underset{\boldsymbol{x}}{\text{maximize}} \quad & F(\boldsymbol{x}), \\ \text{subject to} \quad & \boldsymbol{x} \in \mathcal{D}_1^{(1)} \cap \mathcal{D}_1^{(2)} \end{aligned} \tag{6}$$

where $F(\boldsymbol{x}) = \min\{F^{(1)}(\boldsymbol{x}), F^{(2)}(\boldsymbol{x})\}$ represents the performance of the bottleneck relay channel.

Note that Problem (6) is capable of capturing many applications, e.g., the capacity maximization problem shown in Section 2.2 or wireless charging problem, on the condition that the sub-objective function $f_k^{(i)}(d_i(\boldsymbol{x}))$ is decreasing with the distance $d_i(\boldsymbol{x})$.

In addition, Problem (6) is a non-convex problem mainly due to the arbitrary and non-convex LOS segment $\mathcal{D}_1^{(1)} \cap \mathcal{D}_1^{(2)}$. In particular, this paper studies the optimal UAV placement without the prior geometric information. Therefore, it is almost impossible to solve Problem (6) by conventional optimization approaches.

3 Online search for UAV relay placement

In this section, the solution properties of Problem (6) are demonstrated, which motivate the design of the online search scheme. To solve Problem (6), a special case is first discussed, and then a more general case is studied. Define the strongly line-of-sight (SLOS) segment w.r.t. two users as $\mathcal{D}_1 = \mathcal{D}_1^{(1)} \cap \mathcal{D}_1^{(2)}$ and the weakly non-line-of-sight (WNLOS) segment w.r.t. two users as $\mathcal{D}_2 = \mathcal{D} \backslash \mathcal{D}_1$. Without loss of generality, we assume that the boundary between $\mathcal{D}_1$ and $\mathcal{D}_2$ belongs to $\mathcal{D}_1$. In this paper, WNLOS segment does not contain any feasible relay position due to the significant performance degradation of WNLOS channel in FSO communications.

3.1 Equipotential surface

Define the equipotential surface $\mathcal{M}$ as the region where for each position $\boldsymbol{x} \in \mathcal{M}$, the value of the sub-objective function $f_1^{(1)}(d_1(\boldsymbol{x}))$ of the SR channel equals that of the sub-objective function $f_1^{(2)}(d_2(\boldsymbol{x}))$. Mathematically, $\mathcal{M}$ is specified as

$$\mathcal{M} = \left\{\boldsymbol{x} \in \mathbb{R}^3 | f_1^{(1)}(d_1(\boldsymbol{x})) = f_1^{(2)}(d_2(\boldsymbol{x}))\right\} \tag{7}$$

The following lemma shows the potential of the equipotential plane for Problem (6).

Lemma 1 If $\mathcal{D} = \mathcal{D}_1^{(1)} \cap \mathcal{D}_1^{(2)}$, the optimal solution to Problem (6) is on the equipotential surface $\mathcal{M}$, i.e., $\boldsymbol{x}^* \in \mathcal{M}$.

Proof First, the objective function $F(\boldsymbol{x})$ is degraded to $F(\boldsymbol{x}) = \min\{f_1^{(1)}(d_1(\boldsymbol{x})), f_1^{(2)}(d_2(\boldsymbol{x}))\}$ due to the constraint $\boldsymbol{x} \in \mathcal{D} = \mathcal{D}_1^{(l)} \cap \mathcal{D}_1^{(2)}$. Second, suppose the optimal solution to Problem (6) is not on $\mathcal{M}$. Without loss of generality, one can assume $f_1^{(1)}(d_1(\boldsymbol{x}^*)) > f_1^{(2)}(d_2(\boldsymbol{x}^*))$. Then, there exists a vector $\Delta\boldsymbol{x} \in \mathbb{R}^3$ such that $d_1(\boldsymbol{x}^* + \Delta\boldsymbol{x}) \geqslant d_1(\boldsymbol{x}^*)$ and $d_2(\boldsymbol{x}^* + \Delta\boldsymbol{x}) < d_2(\boldsymbol{x}^*)$, and correspondingly, $f_1^{(1)}(d_1(\boldsymbol{x}^* + \Delta\boldsymbol{x})) \geqslant f_1^{(2)}(d_2(\boldsymbol{x}^* + \Delta\boldsymbol{x})) > f_1^{(2)}(d_2(\boldsymbol{x}^*))$. Thus, $\boldsymbol{x}^* + \Delta\boldsymbol{x}$ is better than $\boldsymbol{x}^*$, which is a contradiction. Finally, $\boldsymbol{x}^*$ must belong to $\mathcal{M}$. ∎

Lemma 1 implies that the optimal solution to Problem (6) potentially lies on the equipotential plane if there is no NLOS regions in the feasible domain $\mathcal{D}$. Even though some of the positions on the equipotential surface are blocked, the SLOS position on the equipotential surface with the largest value of $F(\boldsymbol{x})$ still remains the potentially optimal position. As stated in the proof of Lemma 1, the system performance can be improved for any position $\boldsymbol{x} \in \mathcal{D}_1$ that is not on the

equipotential surface by moving an infinitesimal distance in one of the directions close to the equipotential surface. This implies that there are many local optimal points on or near the equipotential surface when the blockage pattern is considered.

As the SLOS segment $\mathcal{D}_1$ can be arbitrary, it is also valuable to derive another property about the blockage pattern. Denote the closure of the SLOS segment as $\overline{\mathcal{D}}_1$ and the interior of the SLOS segment as $\text{int}(\mathcal{D}_1)$. Then, the boundary of the SLOS region is defined as $\text{bd}(\mathcal{D}_1) = \overline{\mathcal{D}}_1 - \text{int}(\mathcal{D}_1)$.

Lemma 2 The optimal solution to Problem (6) is on the boundary of the SLOS segment, i.e., $\boldsymbol{x}^* \in \text{bd}(\mathcal{D}_1)$.

Proof The proof is completed using contradiction. Suppose the optimal solution $\boldsymbol{x}^*$ is in the interior of the SLOS segment, i.e., $\boldsymbol{x}^* \in \text{int}(\mathcal{D}_1)$. Since the SLOS segment is open, there exists a vector $\Delta\boldsymbol{x} = (0, 0, -\delta)$ where $\delta > 0$ such that $\boldsymbol{x}^* + \Delta\boldsymbol{x} \in \text{int}(\mathcal{D}_1)$. As $f_k^{(i)}(d_i(\boldsymbol{x}))$ is decreasing with $d_i(\boldsymbol{x})$, it holds that $F(\boldsymbol{x}^* + \Delta\boldsymbol{x}) > F(\boldsymbol{x}^*)$, which is a contradiction. Thus, $\boldsymbol{x}^* \in \text{bd}(\mathcal{D}_1)$. ∎

Lemma 2 implies that searching on the boundary of the SLOS segment contributes to finding the optimal relay position. However, the boundary of the SLOS segment can be arbitrary and cannot be obtained without prior map information. Additionally, even the geometric information is available, the complexity of searching on the boundary can also be intolerable. Note that a similar result to Lemma 2 is developed in our prior work[2] but the story is quite different. In Ref. [2], the UAV is deployed to connect a user with a BS and it is assumed that the BS is high enough such that there is always an LOS condition for the BS-UAV link.

3.2 Search on an equipotential plane

As shown in Lemma 1, searching on the equipotential surface $\mathcal{M}$ has the potential to find the globally optimal points or locally optimal points to Problem (6). However, the shape of the equipotential surface may be curved and the complexity of searching on a curved surface is unpractical. Based on this insight, a special case where the equipotential surface turns out to be an equipotential plane is discussed. In particular, one possible example is that the two users in the capacity maximization problem are identical which means that the SR channel and the RD channel share the same channel parameters and transmit power. As for the sub-objective functions $f_1^{(1)}(d_1(\boldsymbol{x}))$ and $f_1^{(2)}(d_2(\boldsymbol{x}))$, it follows that $f_1^{(1)}(d_1(\boldsymbol{x})) \leqslant f_1^{(2)}(d_2(\boldsymbol{x}))$ if and only if $d_1(\boldsymbol{x}) \geqslant d_2(\boldsymbol{x})$, and $f_1^{(1)}(d_1(\boldsymbol{x})) \geqslant f_1^{(2)}(d_2(\boldsymbol{x}))$ if and only if $d_1(\boldsymbol{x}) \leqslant d_2(\boldsymbol{x})$.

In the identical user case, the equipotential plane is the middle perpendicular plane denoted as $\mathcal{M}_0$ between the two users. This can be easily verified because for any position $\boldsymbol{x} \in \mathcal{M}_0$, the distance between $\boldsymbol{x}$ and each user is the same as each other, i.e., $d_1(\boldsymbol{x}) = d_2(\boldsymbol{x})$. Since $f_1^{(1)}(d_1(\boldsymbol{x}))$ and $f_1^{(2)}(d_2(\boldsymbol{x}))$ share the same parameters, it holds that $f_1^{(1)}(d_1(\boldsymbol{x})) = f_1^{(2)}(d_2(\boldsymbol{x}))$ for any position $\boldsymbol{x} \in \mathcal{M}_0$.

For the convenience of the presentation, a Cartesian coordinate system is established by letting the line passing through $\boldsymbol{u}_1$ and $\boldsymbol{u}_2$ be the Y-axis with positive Y-direction being the same as the direction of $\boldsymbol{u}_2 - \boldsymbol{u}_1$, and let the origin be $\boldsymbol{o} = (\boldsymbol{u}_1 + \boldsymbol{u}_2)/2$. The Z-axis is perpendicular to the ground and pointing upward, and the X-axis is determined correspondingly by the right-hand rule as shown in Fig. 1.

Lemma 1 implies the potential of searching on the equipotential plane, i.e., the middle perpendicular plane

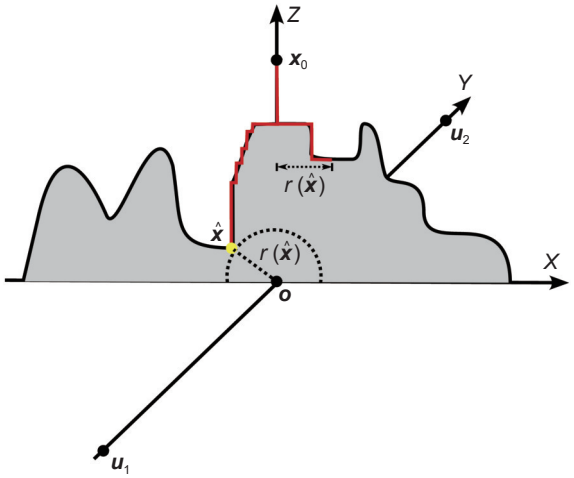

Fig. 1 A UAV acts as a relay between two obstructed and identical users. The equipotential surface is the middle perpendicular plane between the two users. The gray area on the equipotential surface is the WNLOS segment. The red lines represent the proposed search trajectories. It should be noted in particular that during the search in the right half region, the search stops when the *X*-coordinate of the UAV position reaches $r(\hat{x})$ which is the distance between the temporarily best position and the mid-point of the two users.

$\mathcal{M}_0$ in an identical case. Additionally, it is obvious that lowering the UAV position on $\mathcal{M}_0$ will definitely increase the value of the objective function $F(\boldsymbol{x})$ if the new position is SLOS. However, according to the LOS property of the propagation segments shown in Section 2.1, lowering the UAV position increases the degree of signal obstruction. Therefore, when the UAV goes into the WNLOS segment, horizontal movement may be beneficial to increasing the degree of signal obstruction because obstacle occlusion is usually bounded.

To summarize the strategy, the UAV starts from an SLOS position and moves in the negative Z-direction, until it detects the boundary of the SLOS segment. It then moves according to the two possible conditions it detects. If it is in the SLOS segment, it moves in the negative Z-direction until the UAV enters in WNLOS segment. If it is in the WNLOS segment, it moves horizontally on the equipotential plane until the stopping criterion is met, or it enters into the SLOS segment. Denote the distance between the position $\boldsymbol{x} \in \mathcal{M}_0$ and $\boldsymbol{o}$ as

$$r(\boldsymbol{x}) = \|\boldsymbol{x} - \boldsymbol{o}\|_2 \tag{8}$$

Denote the temporarily best position ever found as $\hat{\boldsymbol{x}}$. The following lemma shows that the search should stop when the UAV moves horizontally to a certain point.

Lemma 3 Given the temporarily best position $\hat{\boldsymbol{x}} \in \mathcal{D}$, the inequality $F(\boldsymbol{x}) < F(\hat{\boldsymbol{x}})$ holds for any position $\boldsymbol{x} \in \mathcal{M}_0 \cap \mathcal{D}_1$ satisfying $|x_1| > r(\hat{\boldsymbol{x}})$.

Proof First, for any position $\boldsymbol{x} \in \mathcal{M}_0$, the distance $d_i(\boldsymbol{x})$ can be rewritten as $d_i(\boldsymbol{x}) = \sqrt{{L_i}^2 + r^2(\boldsymbol{x})}$ where $L_i = \|\boldsymbol{u}_i - \boldsymbol{o}\|_2$. Then, for any position $\boldsymbol{x} \in \mathcal{M}_0$ satisfying $|x_1| > r(\hat{\boldsymbol{x}})$,

$$\begin{aligned}&\max\{{d_1}^2(\boldsymbol{x}), {d_2}^2(\boldsymbol{x})\} = r^2(\boldsymbol{x}) + \max\{{L_1}^2, {L_2}^2\} > \\ &r^2(\hat{\boldsymbol{x}}) + \max\{{L_1}^2, {L_2}^2\} = \max\{{d_1}^2(\hat{\boldsymbol{x}}), {d_2}^2(\hat{\boldsymbol{x}})\}\end{aligned} \tag{9}$$

The inequality (9) implies that $F(\boldsymbol{x}) < F(\hat{\boldsymbol{x}})$ since $f_1^{(i)}(d_i(\boldsymbol{x}))$ is decreasing with $d_i(\boldsymbol{x})$. ∎

According to Lemma 3, there is no need to search those SLOS positions on $\mathcal{M}_0$ where the absolute value of the X-coordinate is greater than $r(\hat{\boldsymbol{x}})$, which is a stopping criterion.

Denote the line passing through $\boldsymbol{o}$ and perpendicular to the ground as l_0. The technical details of a two-stage algorithm named TOSEP are shown in Algorithm 1.

Note that the search order of the left and right side of l_0 does not affect the finally resultant relay position of the algorithm. This is because when any of the two stopping criterions is reached, the search will never find a better SLOS position on the search side. Additionally, the best SLOS point found on one side will not be updated until a better SLOS point is found on the other side. The details are shown in the proof of Theorem 1.

Even though the proposed TOSEP has simpler move patterns and stricter stopping criterion than one of the algorithms proposed in our prior work[35], the global optimality on the equipotential plane $\mathcal{M}_0$ is still guaranteed.

Theorem 1 The output $\hat{\boldsymbol{x}}$ of the TOSEP is the optimal relay position on the equipotential plane $\mathcal{M}_0$.

Proof Lemma 3 has demonstrated that any position $\boldsymbol{x} \in \mathcal{M}_0 \cap \mathcal{D}_1$ satisfying $|x_1| > r(\hat{\boldsymbol{x}})$ is worse than $\hat{\boldsymbol{x}}$. Then, one only need to consider those SLOS positions $\boldsymbol{x} \in \mathcal{M}_0 \cap \mathcal{D}_1$ satisfying $|x_1| \leqslant r(\hat{\boldsymbol{x}})$. Suppose the optimal relay position $\boldsymbol{x}^*$ on $\mathcal{M}'$ is not found by the TOSEP. Consider the following two cases.

Case one: Algorithm 1 terminates at a position satisfying $|x_1| < |{x_1}^*|$ and $x_3 = H_{\min}$ on either the left or the right side of l_0. Then, there exists a better SLOS position than $\boldsymbol{x}^*$ due to the smaller distance to $\boldsymbol{o}$ and to both users. Thus, case one does not hold.

Case two: Algorithm 1 terminates at a position satisfying $|x_1| \geqslant |{x_1}^*|$ and $x_3 = H_{\min}$ on either the left or the right side of l_0. Since $\boldsymbol{x}^*$ satisfies ${x_1}^* \leqslant r(\hat{\boldsymbol{x}})$ and ${x_3}^* \geqslant H_{\min}$, $\boldsymbol{x}^*$ is directly below the search trajectory. Otherwise, if $\boldsymbol{x}^*$ is directly above the search trajectory, then there exists an SLOS position $\boldsymbol{x}'$ on the trajectory such that $|x_1'| \leqslant |{x_1}^*|$, $x_3' < {x_3}^*$, and thus, $r(\boldsymbol{x}') < r(\boldsymbol{x}^*)$. This leads to a contradiction because $\boldsymbol{x}'$ is better than $\boldsymbol{x}^*$ while $\boldsymbol{x}^*$ is the optimal solution. Next, since $\boldsymbol{x}^*$ is directly below the search trajectory, the LOS property of the nested propagation segments stated in Section 2.1 shows that there must be an SLOS position $\boldsymbol{x}_1$ directly above $\boldsymbol{x}^*$ on the trajectory. Thus, $\boldsymbol{x}^*$ must be found by searching from $\boldsymbol{x}_1$ downwards, which is a contradiction. Finally, $\boldsymbol{x}^*$ must be found as $\hat{\boldsymbol{x}}$. ∎

Theorem 1 shows that optimal relay position on the equipotential plane is attainable, even though the

terrain topology could be arbitrarily complex.

As for the complexity of the algorithm, it is easy to find that the search trajectory of the TOSEP is only linear in the scale of the target area on the equipotential plane $\mathcal{M}_0$, which results from that the search region is bounded by the minimum search height $H_{\min}$ and the maximum horizontal shift $r(\hat{\boldsymbol{x}})$. Specifically, the following theorem shows the upper bound of the search trajectory length. Denote H_0 as the altitude of the initial SLOS position $\boldsymbol{x}_0$.

Theorem 2 The search trajectory length of the TOSEP is upper bounded by $4H_0 - 2H_{\min}$.

Proof The maximum length of the vertical trajectory and the horizontal trajectory is $2(H_0 - H_{\min})$ and $2H_0$ because of the stopping criterion and the two-stage search. Then, the upper bound of the total length is $4H_0 - 2H_{\min}$. ∎

3.3 Curved equipotential surface in a general case

Consider the general case of Problem (6) where $f_1^{(1)}(d_1(\boldsymbol{x}))$ might be different from $f_1^{(2)}(d_2(\boldsymbol{x}))$. In the capacity maximization problem, for example, the transmit power of User 1 is only 20 dBm while the transmit power of the UAV can be 40 dBm. To maximize the relay capacity of the system, the UAV can move closer to User 1 and thus, improve the performance of the SR channel while the performance of the RD channel can be properly decreased.

Recall that in the identical user case, the equipotential plane is a plane perpendicular to the ground, allowing the obstacles to be projected proportionally to the equipotential surface. More specifically, the shape of the scalable projection on the equipotential surface is identical to the shape of the obstacle side facing the corresponding user, with the only difference being that the projection is larger in size than the real obstacle side facing the user. The LOS property of the nested propagation segments stated in Section 2.1 holds on the perpendicular plane because of the scale-up projection with the same geometric shape.

In the general case, the equipotential surface may no longer be a perpendicular plane between two users. Instead, M corresponds to a curved surface, washing over one of the two users like a tsunami, and extending to the sky behind this user. Consider the case where the equipotential surface is not a perpendicular plane. Lowering the altitude of UAV with a fixed X-coordinate may cause it to alternate between SLOS and WNLOS conditions because the projection of the obstacles on the equipotential surface is different from the real obstacle side facing the user in terms of shape and size. Therefore, the LOS property of the nested propagation segments cannot be guaranteed to hold on the curved surface.

3.4 Approximated search strategy in a general case

To make the LOS property of the nested propagation segments mentioned in Section 2.1 hold, it is natural to approximate the curved equipotential surface to a plane perpendicular to the ground.

To reduce the computation cost, it is not necessary to approximate the whole equipotential surface as a perpendicular plane. A cost-friendly strategy is to approximate a critical part of the equipotential surface as a perpendicular plane to the ground. Without loss of generality, consider the part of the equipotential surface where the Y-component of all the positions is greater than or equal to zero. As shown in Fig. 2, the critical part of the equipotential surface is defined as

$$\widetilde{\mathcal{M}} \triangleq \left\{\boldsymbol{x} \in \mathcal{M} | 0 \leqslant x_2 \leqslant x_2^{\text{tot}}\right\} \tag{10}$$

where x_2^{tot} is the Y-coordinate of the point $\boldsymbol{x}^{\text{tot}}$ which is the intersection point between the equipotential surface $\mathcal{M}$ and the line segment joining $\boldsymbol{u}_1$ and $\boldsymbol{u}_2$. Specifically, $\boldsymbol{x}^{\text{tot}}$ can be obtained by solving the following equations.

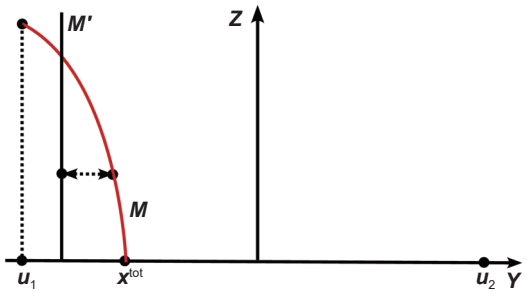

Fig. 2 Approximated perpendicular plane $\mathcal{M}'$. The equipotential plane $\mathcal{M}$ represented by the red curve is approximated as a perpendicular plane $\mathcal{M}'$.

$$\begin{cases} f_1^{(1)}(d_1(\boldsymbol{x})) = f_1^{(2)}(d_2(\boldsymbol{x})), \\ x_1 = 0, \\ x_3 = 0 \end{cases} \tag{11}$$

Let $\mathcal{M}_{1,3} = \{(x_1, x_3) \in \mathbb{R}^2 | (x_1, x_2, x_3) \in \widetilde{\mathcal{M}}\}$. Then, define the approximated perpendicular plane as

$$\mathcal{M}' = \{\boldsymbol{x} \in \mathbb{R}^3 | x_2 = a^*\} \tag{12}$$

where a^* is the solution to the following problem

$$\begin{aligned} \underset{a}{\text{mininize}} \quad & \iint_{(x_1,x_3)\in\mathcal{M}_{1,3}} \frac{1}{2}\|\boldsymbol{x}' - \boldsymbol{x}\|^2 \mathrm{d}x_1 \mathrm{d}x_3, \\ \text{subject to} \quad & 0 \leqslant a \leqslant {x_2}^{\text{tot}}, \\ & \boldsymbol{x}' = (x_1, a, x_2) \in \mathcal{M}', \\ & \boldsymbol{x} = (x_1, x_2, x_3) \in \tilde{\mathcal{M}} \end{aligned} \tag{13}$$

Problem (13) approximately captures the distance between the approximated perpendicular plane $\mathcal{M}'$ and a critical part of the equipotential surface $\mathcal{M}$. It is found that Problem (13) can be further simplified and specified as

$$\begin{aligned} \underset{a}{\text{minimize}} \quad & G(a), \\ \text{subject to} \quad & 0 \leqslant a \leqslant {x_2}^{\text{tot}}, \\ & (x_1, x_2, x_3) \in \widetilde{\mathcal{M}} \end{aligned} \tag{14}$$

where $G(a) = \iint_{(x_1,x_3)\in\mathcal{M}_{1,3}} \frac{1}{2}(a - x_2)^2 \mathrm{d}x_1 \mathrm{d}x_3$. Problem (14) is a convex problem since $G(a)$ is convex w.r.t. a, and the constraints of a are linear, and thus, convex. Given the box constraints of a, i.e., $\mathcal{Q} = \{a \in \mathbb{R} | 0 \leqslant a \leqslant {x_2}^{\text{tot}}\}$, define a projection onto the convex set $\mathcal{Q}$ as

$$P_{\mathcal{Q}}(a) = \begin{cases} 0, & a < 0; \\ a, & 0 \leqslant a \leqslant x_2^{\text{tot}}; \\ x_2^{\text{tot}}, & a > x_2^{\text{tot}} \end{cases} \tag{15}$$

Then, one can use the gradient projection method to solve Problem (14) and obtain the optimal solution a^*.

Given the approximated perpendicular plane $\mathcal{M}'$, the proposed TOSEP can be executed except for the initialization. Define a point $\boldsymbol{o}'$ as the intersection point between the approximated equipotential plane $\mathcal{M}'$ and the line segment joining $\boldsymbol{u}_1$ and $\boldsymbol{u}_2$. Note that an SLOS position perpendicularly above $\boldsymbol{o}'$ can always be found if the UAV flies high enough according to the LOS property of the nested propagation segments mentioned in Section 2.1. The technical details of the algorithm named GOSAEP for the general case are shown in Algorithm 2.

Algorithm 2 GOSAEP

Input: User positions $\boldsymbol{u}_1$ and $\boldsymbol{u}_2$, a search step size μ, stopping criterion ϵ, and a optimization step size γ_0.

Output: The optimal relay position $\tilde{\boldsymbol{x}}$.

1. Calculate the boundary point $\boldsymbol{x}^{\text{tot}}$ by solving Eq. (11).
2. Calculate the optimal solution a^* to Problem (14) using a gradient projection method.
   (1) Initialize $a^{(0)} = {x_2}^{\text{tot}}/2$ and $j = 0$.
   (2) Pick a descent direction as
   $$-\nabla G(a^{(j)}) = -\iint_{(x_1,x_3)\in\mathcal{M}_{1,3}} (a^{(j)} - x_2)\mathrm{d}x_1\mathrm{d}x_3.$$
   (3) Pick a step size γ according to the backtracking line search method.
   (a) Initialize $\gamma = \gamma_0$.
   (b) Until $G(P_{\Omega}(a - \gamma \cdot \nabla G(a))) < G(a)$:
   Set $\gamma = \tau \cdot \gamma$ where $\tau \in (0, 1)$.
   (4) Update: $a^{(j+1)} \leftarrow P_{\Omega}(a^{(j)} - \gamma \cdot \nabla G(a))$ and $j \leftarrow j + 1$.
   (5) Repeat Steps (2)–(4) until $\left|a^{(j)} - a^{(j-1)}\right| < \epsilon$.
3. Define a perpendicular plane
   $$\mathcal{M}' = \{\boldsymbol{x} \in \mathbb{R}^3 | x_2 = a^{(j)}\}.$$
4. Find an initial SLOS position above $\boldsymbol{o}'$, execute the TOSEP on $\mathcal{M}'$, and output $\tilde{\boldsymbol{x}}$.

The proposed GOSAEP also has a linear search trajectory length because the main idea of the GOSAEP is to find an approximated equipotential plane $\mathcal{M}'$ and then apply the TOSEP to $\mathcal{M}'$.

Define a simplified version of Problem (6) as

$$\begin{aligned} \underset{\boldsymbol{x}}{\text{maximize}} \quad & F(\boldsymbol{x}), \\ \text{subject to} \quad & \boldsymbol{x} \in \mathcal{D}_1^{(1)} \cap \mathcal{D}_1^{(2)} \cap \mathcal{M}' \end{aligned} \tag{16}$$

Problem (16) differs from Problem (6) in that Problem (16) limits the 3D search space of Problem (6) to a well-designed 2D plane. Although it is hard to reach global optimality in 3D space, the GOSAEP is capable of achieving global optimality on the 2D perpendicular plane $\mathcal{M}'$.

Theorem 3 The output $\tilde{\boldsymbol{x}}$ of the GOSAEP is the optimal solution to Problem (16).

Proof The proof can be completed by adopting the proof methods of Theorem 1 and Lemma 3. ∎

4 Numerical experiment

4.1 Propagation environment

The experiments are conducted over a real 3D city map shown in Fig. 3. The total area of the map is 2000 m × 2000 m. The building coverage ratio (BCR)[37]

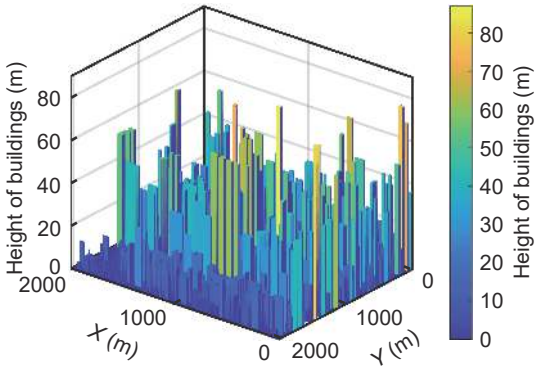

Fig. 3 A 3D map of a local area in Beijing, China.

is used to quantify the building density of this map. Specifically, the BCR of this area is 32%. It is observed from Fig. 3 that the buildings are quite dense in this area, and thus, the transmission signal is easily to be blocked. As for FSO communications, a UAV relay is strongly needed to construct LOS links with two users in the deep shadow. Since the maximum height of the buildings in this area is 87 m, the minimum flying height of the UAV is set as 87 m to avoid any potential collision.

To evaluate the performance of the proposed algorithms, 1000 pairs of users are randomly located at the area where there is no building. In addition, the inter-user distance is set to be greater than 500 m such that the direct inter-user link performs much worse than the UAV relay link. In this case, UAV relaying is extremely needed.

For the UAV relay system in FSO communications, the channel parameters stated in Section 2.2 are set as $\beta_0 = -46.43$ dB, and $\alpha_0 = 2$[20]. The allocated bandwidth of the SR channel and the RD channel is set as $W_s = W_r = 1$ MHz. The noise power spectrum density is set as −174 dBm/Hz.

4.2 Baseline schemes and settings of the propose algorithms

The baseline schemes are listed below.

(1) **Exhaustive 3D search:** This scheme performs exhaustive 3D search over the area of interest with a step size of 5 m.

(2) **Statistical method:** This scheme models the channel gain based on the probability of UAV position belonging to LOS or NLOS region. According to Refs. [36, 38], the channel gain is defined as

$$g_{\text{sta}} = \Pr_{\text{los}}(\boldsymbol{x}) \times \beta_0 / d_i(\boldsymbol{x})^{\alpha_0} + (1 - \Pr_{\text{los}}(\boldsymbol{x})) \times \beta_1 / d_i(\boldsymbol{x})^{\alpha_1},$$

where α_1 and β_1 are channel parameters of the NLOS link, and $\Pr_{\text{los}}(\boldsymbol{x})$ is the LOS probability of the position $\boldsymbol{x}$, which is affected by the elevation angle of the UAV position. The LOS probability $\Pr_{\text{los}}(\boldsymbol{x})$ is defined as

$$\Pr_{\text{los}}(\boldsymbol{x}) = \frac{1}{1 + \eta_1 \times \mathrm{e}^{-\eta_2\left(\arctan\left(x_3 / \sqrt{\|\boldsymbol{x}-\boldsymbol{u}_i\|^2 - x_3^2}\right) - \eta_1\right)}},$$

where η_1 and η_2 are the environment parameters corresponding to the actual distribution of LOS regions. In the experiments, the channel parameters α_1 and β_1 are set as $\beta_1 = -56.43$ dB, and $\alpha_1 = 3.3$[20], providing great signal attenuation in FSO communications if the UAV-user link is NLOS. The environment parameters η_1 and η_2 are learned from the actual map data as 58.91 and 8.90, respectively.

As for the proposed algorithms, the search step size μ is set as 5 m. The stopping criterion ϵ is set as 1 m, and the optimization step size γ_0 is set as $1/\|\boldsymbol{u}_1 - \boldsymbol{u}_2\|_2$.

4.3 Numerical results

Figure 4 shows the capacity of the UAV relay system in an identical user case. Both the transmit powers of User 1 and the UAV are set as 40 dBm. After sorting the test cases by channel capacity, the mean value of the capacities of the best 20%, the worst 20%, and all of the test cases are compared. First, it is observed that the proposed TOSEP and GOSAEP achieve the same performance, i.e., mean capacity, in the identical user case. This results from that the equipotential surface $\mathcal{M}$

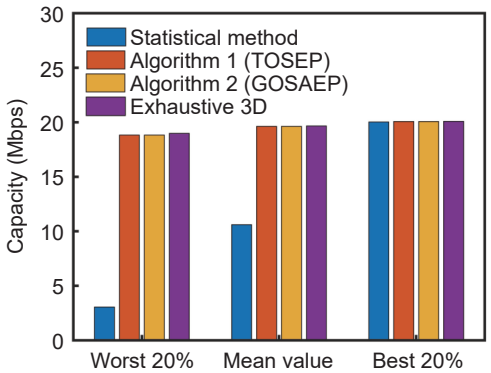

Fig. 4 Performance of the UAV relay system in an identical user case where the transmit power of both the UAV and User 1 is set to 40 dBm.

is exactly the middle perpendicular plane $\mathcal{M}_0$ in this case, and correspondingly, the approximated equipotential plane $\mathcal{M}'$ of the GOSAEP obtained by solving Problem (14) is also the middle perpendicular plane $\mathcal{M}_0$. Second, regardless of the performance of the worst 20% of test cases, the performance of the best 20% of test cases, or the average performance, both the TOSEP and GOSAEP approximate the performance of the exhaustive 3D search scheme. Specifically, both the TOSEP and GOSAEP achieve over 99% to the performance of the exhaustive 3D search scheme.

In addition, it is observed in Fig. 4 that the statistical method finds good solutions for the best 20% of test cases sorted by capacity. However, it only reaches about 16% of the performance of the exhaustive 3D search scheme for the worst 20% of test cases, and about 54% optimality considering all the test cases. This is because the statistical method does not guarantee the LOS condition of the optimal position obtained from its offline exhaustive search. In the FSO communications, the capacity of the relay link will be greatly reduced if the optimal position found by the statistical method is WNLOS.

Figure 5 depicts the capacity of the UAV relay system in a non-identical case. The transmit power of User 1 is set to 15 dBm while the transmit power of the UAV is set to 40 dBm. Under this setting, the performance gain of the GOSAEP over the TOSEP is obvious, especially for the best 20% test cases. Specifically, the GOSAEP achieves over 99% of the performance of the exhaustive 3D search scheme while the TOSEP only achieves about 80% of the performance of the exhaustive 3D search scheme. This results from the potential of the equipotential surface stated in Lemma 1. When the difference in transmission power is large, the equipotential surface will favor the side of the user served by the link with less transmission power. The GOSAEP is capable of finding the positions that make the length of the poorer relay link smaller since it searches on a perpendicular plane as close as possible to the equipotential surface. Additionally, it is found that the statistical method performs worse in the non-identical case compared with its performance shown in Fig. 4. This implies that the statistical method considering only the elevation angle of the UAV position is not practical.

Figure 6 depicts the mean capacity of the UAV relay system under different transmit powers of User 1 while the transmit power of the UAV is set to 40 dBm. In this experiment, the transmit power of User 1 determines the degree of link asymmetry. Specifically, when the transmit power of User 1 is close to that of the UAV, the degree of link asymmetry is small. Otherwise, greater difference between the transmit power of User 1 and that of the UAV leads to greater degree of link asymmetry. It is found from the curves in Fig. 6 that, the GOSAEP achieves near-optimal performance, i.e., over 95% to the exhaustive 3D search scheme, at all the tested degrees of link asymmetry. In addition, when

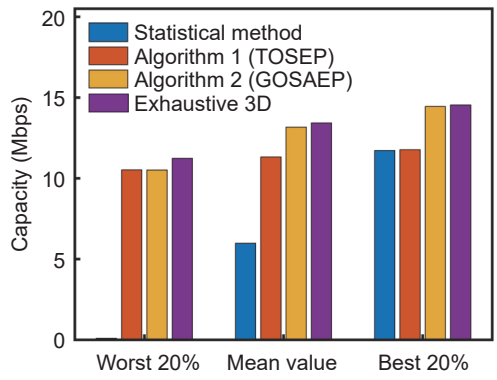

Fig. 5 Performance of the UAV relay system in a non-identical case where the transmit power of User 1 is set as 15 dBm while the transmit power of the UAV is set as 40 dBm.

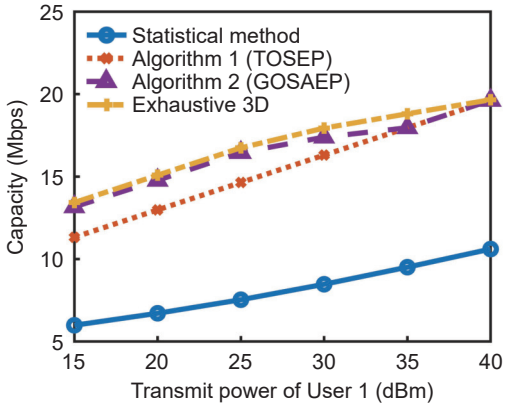

Fig. 6 Performance of the UAV relay system under different degrees of link asymmetry determined by the difference between the transmit power of User 1 and that of the UAV.

the degree of link asymmetry becomes smaller, i.e., when the transmit power of User 1 is 35 or 40 dBm, the performance of the TOSEP gets closer to that of the GOSAEP.

Table 1 shows the average trajectory length of proposed algorithms under different degrees of link asymmetry. It is observed that the proposed algorithms can find a near-optimal solution within a search distance of 200−300 m while the search trajectory length of the exhaustive 3D search scheme is about 15−30 km.

5 Conclusion

This paper studied the UAV relay placement problem in an FSO communication system composed of two static and obstructed users. Unlike most of the past works, the actual terrain structure, which may have irregular and arbitrary shapes, was considered and it was assumed that there was no prior geometric information before search. To solve the problem, two solution properties were first demonstrated. It was shown that the globally optimal relay position in 3D space potentially lied on the equipotential surface, with the objective function being the smaller utility of the two users, and the optimal relay position was on the boundary of the SLOS segment. Motivated by the two solution properties, an efficient algorithm named TOSEP was developed. If the two served users were identical, the equipotential surface was an equipotential plane perpendicular to the ground while the equipotential surface was curved in a general case. To search as close as possible to the equipotential surface, a gradient projection method was adopted to approximate the equipotential surface as a perpendicular plane so that the TOSEP can run on it. It was claimed that the proposed algorithms achieved global optimality on the search plane. The experiments were conducted on real map data. It was found that the proposed GOSAEP reached over 95% of performance of the exhaustive 3D search scheme within a search distance of 300 m in all the tested cases.

Table 1 Average trajectory length of proposed algorithms under different degrees of link asymmetry.

P_s (dBm)	Average trajectory length (m)	
	TOSEP	GOSAEP
15	190	244
20	190	237
25	190	260
30	190	260
35	190	260
40	190	193

Acknowledgment

This work was supported in part by the National Key R&D Program of China (No. 2018YFB1800800), the Basic Research Project of Hetao Shenzhen-HK S&T Cooperation Zone (No. HZQB-KCZYZ-2021067), National Natural Science Foundation of China (Nos. 62171398 and 92067202), the Shenzhen Science and Technology Program (Nos. JCYJ20210324134612033 and KQTD20200909114730003), Guangdong Research (Nos. 2019QN01X895 and 2017ZT07X152), and Guangdong Provincial Key Laboratory of Future Networks of Intelligence (No. 2022B1212010001).

References

[1] M. T. Dabiri, S. Khankalantary, M. J. Piran, I. S. Ansari, M. Uysal, W. Saad, and C. S. Hong, UAV-assisted free space optical communication system with amplify-and-forward relaying, *IEEE Trans. Vehicular Tech.*, vol. 70, no. 9, pp. 8926–8936, 2021.

[2] J. Chen and D. Gesbert, Efficient local map search algorithms for the placement of flying relays, *IEEE Trans. Wireless Commun.*, vol. 19, no. 2, pp. 1305–1319, 2020.

[3] M. T. Dabiri and S. M. S. Sadough, Performance analysis of all-optical amplify and forward relaying over log-normal FSO channels, *J. Opt. Commun. Netw.*, vol. 10, no. 2, pp. 79–89, 2018.

[4] Y. Kaymak, R. Rojas-Cessa, J. Feng, N. Ansari, M. Zhou, and T. Zhang, A survey on acquisition, tracking, and pointing mechanisms for mobile free-space optical communications, *IEEE Commun. Surv. Tutor.*, vol. 20, no. 2, pp. 1104–1123, 2018.

[5] A. Jahid, M. H. Alsharif, and T. J. Hall, A contemporary survey on free space optical communication: Potentials, technical challenges, recent advances and research direction, *J. Netw. Comput. Appl.*, vol. 200, pp. 1–35, 2022.

[6] J. Chen, U. Yatnalli, and D. Gesbert, Learning radio maps for UAV-aided wireless networks: A segmented regression approach, in *Proc. IEEE Int. Conf. Commum.*,

Paris, France, 2017, pp. 1–6.

[7] J. Lee, K. Park, M. Alouini, and Y. Ko, Free space optical communication on UAV-assisted backhaul networks: Optimization for service time, in *Proc. 2019 IEEE Globecom Workshops* (*GC Wkshps*), Waikoloa, HI, USA, 2019, pp. 1–6.

[8] J. Chen, O. Esrafilian, D. Gesbert, and U. Mitra, Efficient algorithms for air-to-ground channel reconstruction in UAV-aided communications, in *Proc. 2017 IEEE Globecom Workshops* (*GC Wkshps*), Singapore, 2017, pp. 1–6.

[9] J. Chen, U. Mitra, and D. Gesbert, 3D urban UAV relay placement: Linear complexity algorithm and analysis, *IEEE Trans. Wireless Commun.*, vol. 20, no. 8, pp. 5243–5257, 2021.

[10] J. Chen and U. Mitra, Data clustering using matrix factorization techniques for wireless propagation map reconstruction, in *Proc. IEEE Statical Signal Process. Workshop*, Freiburg im Breisgau, Germany, 2018, pp. 856–860.

[11] J. Lyu, Y. Zeng, and R. Zhang, Cyclical multiple access in UAV-aided communications: A throughput-delay tradeoff, *IEEE Wireless Commun. Lett.*, vol. 5, no. 6, pp. 600–603, 2016.

[12] Q. Wu and R. Zhang, Common throughput maximization in UAV-enabled OFDMA systems with delay consideration, *IEEE Trans. Wireless Commun.*, vol. 66, no. 12, pp. 6614–6627, 2018.

[13] Q. Wu and R. Zhang, Delay-constrained throughput maximization in UAV-enabled OFDM systems, in *Proc. IEEE Asia–Pacific Conf. Commun.* (*APCC*), Perth, Australia, 2017, pp. 1–6.

[14] V. V. Chetlur and H. S. Dhillon, Downlink coverage analysis for a finite 3-D wireless network of unmanned aerial vehicles, *IEEE Trans. Commun.*, vol. 65, no. 10, pp. 4543–4558, 2017.

[15] J. Lyu, Y. Zeng, R. Zhang, and T. J. Lim, Placement optimization of UAV-mounted mobile base stations, *IEEE Commun. Lett.*, vol. 21, no. 3, pp. 604–607, 2017.

[16] Q. Wu, J. Xu, and R. Zhang, Capacity characterization of UAV-enabled two-user broadcast channel, *IEEE J. Sel. Areas Commun.*, vol. 36, no. 9, pp. 1955–1971, 2018.

[17] Q. Wu, J. Xu, and R. Zhang, UAV-enabled broadcast channel: Trajectory design and capacity characterization, in *Proc. IEEE Int. Conf. Commun.* (*ICC*) *Workshops*, Kansas City, MO, USA, 2018, pp. 1–6.

[18] B. Galkin, J. Kibiłda, and L. A. DaSilva, A stochastic model for UAV networks positioned above demand hotspots in urban environments, *IEEE Trans. Veh. Technol.*, vol. 68, no. 7, pp. 6985–6996, 2019.

[19] B. Galkin, J. Kibiłda, and L. A. DaSilva, Coverage analysis for low-altitude UAV networks in Urban environments, in *Proc. IEEE Global Commun. Conf.*, Singapore, 2017, pp. 1–6.

[20] P. Yi, L. Zhu, L. Zhu, Z. Xiao, Z. Han, and X. Xia, Joint 3-D positioning and power allocation for UAV relay aided by geographic information, *IEEE Trans. on Wireless Commun.*, vol. 21, no. 10, pp. 8148–8162, 2022.

[21] Y. Wu, S. Wu, and X. Hu, Multi-constrained cooperative path planning of multiple drones for persistent surveillance in urban environments, *Complex Intell. Syst.*, no. 7, pp. 1633–1647, 2021.

[22] G. Zhang, Q. Wu, M. Cui, and R. Zhang, Securing UAV communications via joint trajectory and power control, *IEEE Trans. Wireless Commun.*, vol. 18, no. 2, pp. 1376–1389, 2019.

[23] H. Wang, J. Wang, G. Ding, J. Chen, Y. Li, and Z. Han, Spectrum sharing planning for full-duplex UAV relaying systems with underlaid D2D communications, *IEEE J. Select. Areas Commun.*, vol. 36, no. 9, pp. 1986–1999, 2018.

[24] M. K. Samimi, T. S. Rappaport, and G. R. MacCartney, Probabilistic omnidirectional path loss models for millimeter-wave outdoor communications, *IEEE Wireless Commun. Lett.*, vol. 4, no. 4, pp. 357–360, 2015.

[25] O. Esrafilian, R. Gangula, and D. Gesbert, Learning to communicate in UAV-aided wireless networks: Map-based approaches, *IEEE Internet Things J.*, vol. 6, no. 2, pp. 1791–1802, 2019.

[26] M. Chen, M. Mozaffari, W. Saad, C. Yin, M. Debbah, and C. S. Hong, Caching in the sky: Proactive deployment of cache-enabled unmanned aerial vehicles for optimized quality-of-experience, *IEEE J. Sel. Areas Commun.*, vol. 35, no. 5, pp. 1046–1061, 2017.

[27] I. Bor-Yaliniz, S. S. Szyszkowicz, and H. Yanikomeroglu, Environment-aware drone-base-station placements in modern metropolitans, *IEEE Wireless Commun. Lett.*, vol. 7, no. 3, pp. 372–375, 2018.

[28] Y. Chen and D. Huang, Joint trajectory design and BS association for cellular-connected UAV: An imitation-augmented deep reinforcement learning approach, *IEEE Internet Things J.*, vol. 9, no. 4, pp. 2843–2858, 2022.

[29] M. Mozaffari, W. Saad, M. Bennis, and M. Debbah, Drone small cells in the clouds: Design, deployment and performance analysis, in *Proc. 2015 IEEE Global Telecom. Conf.* (*GLOBECOM*), San Diego, CA, USA, 2015, pp. 1–6.

[30] J. Chen, U. Yatnalli, and D. Gesbert, Learning radio maps for UAV-aided wireless networks: A segmented regression approach, in *Proc. IEEE Int. Conf. Commun.*, Paris, France, 2017, pp. 1–6.

[31] Y. Dong, C. He, Z. Wang, and L. Zhang, Radio map

assisted path planning for UAV anti-jamming communications, *IEEE Signal Process. Lett.*, vol. 29, pp. 607–611, 2022.

[32] A. Liu and V. K. N. Lau, Optimization of multi-UAV-aided wireless networking over a ray-tracing channel model, *IEEE Trans. Wireless Commun.*, vol. 18, no. 9, pp. 4518–4530, 2019.

[33] J. Zhao, J. Liu, J. Jiang, and F. Gao, Efficient deployment with geometric analysis for mmwave UAV communications, *IEEE Wireless Commun. Lett.*, vol. 9, no. 7, pp. 1115–1119, 2020.

[34] O. Esrafilian, R. Gangula, and D. Gesbert, Three-dimensional-map-based trajectory design in UAV-aided wireless localization systems, *IEEE Internet Thing J.*, vol. 8, no. 12, pp. 9894–9904, 2021.

[35] Y. Zheng and J. Chen, Geography-aware optimal UAV 3D placement for LOS relaying: A geometry approach, arXiv preprint arXiv: 2209.15161, 2022.

[36] A. Al-Hourani, S. Kandeepan, and S. Lardner, Optimal LAP altitude for maximum coverage, *IEEE Wireless Commun. Lett.*, vol. 3, no. 6, pp. 569–572, 2014.

[37] D. Gonzalez-Aguilera, E. Crespo-Matellan, D. Hernandez-Lopez, and P. Rodriguez-Gonzalvez, Automated urban analysis based on LiDAR-derived building models, *IEEE Trans. Geosci. Remote Sens.*, vol. 51, no. 3, pp. 1844–1851, 2013.

[38] P. Kumar, P. Singh, S. Darshi, and S. Shailendra, Analysis of drone assisted network coded cooperation for next generation wireless network, *IEEE Trans. Mob. Comput.*, vol. 20, no. 1, pp. 93–103, 2021.

Junting Chen received the PhD degree in electronic and computer engineering from Hong Kong University of Science and Technology (HKUST) in 2015, and the BSc degree in electronic engineering from Nanjing University in 2009. During 2014−2015, he was a visiting student with the Wireless Information and Network Sciences Laboratory at MIT, Cambridge, MA, USA. He is an assistant professor with the School of Science and Engineering and the Future Network of Intelligence Institute (FNii), The Chinese University of Hong Kong, Shenzhen (CUHK-Shenzhen), Guangdong, China. Prior to joining CUHK-Shenzhen, he was a postdoctoral research associate with the Ming Hsieh Department of Electrical Engineering, University of Southern California (USC), Los Angeles, CA, USA, during 2016−2018, and with the Communication Systems Department of EURECOM, Sophia-Antipolis, France, during 2015−2016. His research interests include channel estimation, MIMO beamforming, machine learning, and optimization for wireless communications and localization. His current research focuses on radio map sensing, construction, and application for wireless communications. He was a recipient of the HKTIIT Post-Graduate Excellence Scholarships in 2012. He was nominated as the Exemplary Reviewer of *IEEE Wireless Communications Letters* in 2018. His paper received the Charles Kao Best Paper Award from WOCC 2022.

Yuanshuai Zheng received the BEng degree from University of Electronic Science and Technology of China, Chengdu, China, in 2020. He is currently pursuing the PhD degree with the School of Science and Engineering, The Chinese University of Hong Kong, Shenzhen, China. His research interests include UAV-aided communications and networking.

Yinjun Wang is currently pursuing the BS degree at The Chinese University of Hong Kong, Shenzhen. He is interested in optimization, machine learning, and statistics.